Rho is Required for the Initiation of Calcium Signaling and Phagocytosis by Fcγ Receptors in Macrophages

By David J. Hackam,*‡ Ori D. Rotstein,‡ Alan Schreiber,§ Wei-jian Zhang,*‡ and Sergio Grinstein*

*From the *Division of Cell Biology, Hospital for Sick Children, Toronto, Ontario, M5G 1X8, Canada; ‡Department of Surgery, The Toronto Hospital, Toronto, Ontario, M5G 2C4, Canada; and §Department of Medicine, University of Pennsylvania School of Medicine, Philadelphia, Pennsylvania 19104-4283*

Summary

Phagocytosis of bacteria by macrophages and neutrophils is an essential component of host defense against infection. The mechanism whereby the interaction of opsonized particles with Fcγ receptors triggers the engulfment of opsonized particles remains incompletely understood, although activation of tyrosine kinases has been recognized as an early step. Recent studies in other systems have demonstrated that tyrosine kinases can in turn signal the activation of small GTPases of the ras superfamily. We therefore investigated the possible role of Rho in Fc receptor–mediated phagocytosis. To this end we microinjected J774 macrophages with C3 exotoxin from *Clostridium botulinum*, which ADP-ribosylates and inactivates Rho. C3 exotoxin induced the retraction of filopodia, the disappearance of focal complexes, and a global decrease in the F-actin content of J774 cells. In addition, these cells exhibited increased spreading and the formation of vacuolar structures. Importantly, inactivation of Rho resulted in the complete abrogation of phagocytosis. Inhibition of Fcγ receptor–mediated phagocytosis by C3 exotoxin was confirmed in COS cells, which become phagocytic upon transfection of the FcγRIIA receptor. Rho was found to be essential for the accumulation of phosphotyrosine and of F-actin around phagocytic cups and for Fcγ receptor–mediated Ca^{2+} signaling. The clustering of receptors in response to opsonin, an essential step in Fcγ-induced signaling, was the earliest event shown to be inhibited by C3 exotoxin. The effect of the toxin was specific, since clustering and internalization of transferrin receptors were unaffected by microinjection of C3. These data identify a role for small GTPases in Fcγ receptor–mediated phagocytosis by leukocytes.

Phagocytosis of microorganisms by leukocytes is an important component of the host defense against infection (1). Opsonization of bacteria and other particles with antibodies greatly facilitates the phagocytic process and recent studies have contributed greatly to the characterization of the receptors involved and their mode of signaling (for review see reference 2). Upon attachment of opsonized particles to the cell surface, nonreceptor tyrosine kinases induce phosphorylation of the Fcγ receptors, a process which in turn promotes the recruitment and clustering of p72syk. Clustering of this tyrosine kinase appears to be a crucial step in the initiation of phagocytosis (3), and is accompanied by an accumulation of additional phosphorylated proteins at the cell surface and a rise in free cytoplasmic Ca^{2+} (2, 4). These events culminate in the formation of an actin-rich cup around the nascent phagosome and the internalization of the particle (5–7). While individual components of this process have been studied, the molecular mechanisms coordinating the events at the cell surface with the subsequent cytoskeletal rearrangements resulting in phagocytosis remain largely unexplained.

Recent studies in other biological systems have demonstrated that alterations in the actin cytoskeleton in response to extracellular signals are mediated by a family of small GTP-binding proteins (8–12). One member of this family, the GTPase Rho, stabilizes the focal plaques which form at sites of attachment of cells to the substratum and promotes the generation of stress fibers (13). Such attachment is generally mediated by integrins, a group of heterodimeric transmembrane glycoproteins (14). Upon interaction with the extracellular matrix, integrins cluster within the membrane, initiating a signaling sequence which involves tyrosine phosphorylation and the formation of focal adhesions. The latter serve as a scaffold for the assembly of a number of signal transducing molecules, including mitogen-activated protein kinases (15), and provide an anchor-

 J. Exp. Med. © The Rockefeller University Press • 0022-1007/97/09/955/12 $2.00
Volume 186, Number 6, September 15, 1997 955–966
http://www.jem.org

ing site for stress fibers. Importantly, Rho is required for integrin clustering and the subsequent generation of signals which culminates in cytoskeletal rearrangement.

In an analogous fashion, Rho may play a role in signaling the cytoskeletal remodeling in phagocytes in response to bacterial attachment, leading ultimately to bacterial ingestion. In this study, this possibility was addressed experimentally by treating murine macrophages (J774) with the C3 exotoxin of *Clostridium botulinum*. This toxin catalyzes the ADP ribosylation of Rho, resulting in the selective functional inactivation of this GTP-binding protein (16). C3 exotoxin, which enters cells very poorly, was introduced into the macrophages by microinjection. This required the implementation of microfluorescence ratio imaging and video microscopy to evaluate the role of Rho in phagosomal formation and acidification at the single cell level. Using this approach, this study demonstrated that Rho plays a permissive role in the events leading to phagocytosis.

Materials and Methods

Materials, Solutions, and Antibodies

Nigericin, FITC, zymosan A, fura dextran (potassium salt, 10,000 mol wt), fluorescein dextran, fura-2 acetoxymethylester, Lucifer yellow, Texas red–labeled human transferrin, and rhodamine phalloidin were from Molecular Probes Inc. (Eugene, OR). C3 exotoxin from *C. botulinum* was from List Biological Laboratories (Campbell, CA). Fibronectin, 3-μm diameter latex particles, donkey serum, cytochalasin D, and Hepes-buffered medium RPMI were obtained from Sigma Chemical Co. (St. Louis, MO). Human IgG was from Baxter Healthcare Corp. (Glendale, CA). Mouse antiphosphotyrosine cocktail, containing equivalent amounts of the antiphosphotyrosine monoclonal antibodies PY-7E1, PY-1B2, and PY-20, was obtained from Zymed Laboratories (South San Francisco, CA). Rat anti–mouse CD32/CD16 (FcγII/III receptor) monoclonal antibody was obtained from PharMingen (San Diego, CA). Anti-Cy3–conjugated donkey anti–mouse IgG and anti–rat IgG were obtained from Jackson ImmunoResearch Laboratories (West Grove, PA).

PBS consisted of (mM): 140 NaCl, 10 KCl, 8 sodium phosphate, 2 potassium phosphate, pH 7.4. Microinjection buffer consisted of (mM): 110 potassium acetate, 20 NaCl, 10 Hepes, 2 $MgCl_2$, 1 dithiothreitol, pH 7.2. Experiments for determination of free cytosolic calcium $[Ca^{2+}]_i$[1] were performed in medium containing (mM): 127 NaCl, 5 KCl, 2 $MgCl_2$, 2 $CaCl_2$, 5 $NaHCO_3$, 10 Hepes-NaOH, 10 glucose, pH 7.4. In the Ca^{2+}-free medium, $CaCl_2$ was replaced with 5 mM EGTA.

Cell Culture and Handling

The murine cell line J774 and the hybridoma generating the pan anti–MHC I monoclonal antibody were obtained from American Type Culture Collection (Rockville, MD). COS-1 cells, derived from monkey kidney, were stably transfected with FcγRIIA cDNA as described (17). Both cell lines were maintained in DMEM with 10% fetal bovine serum and 5% penicillin-streptomycin (Life Technologies, Grand Island, NY) and incubated at 37°C under 5% CO_2. Before microinjection, cells were plated overnight on acid-washed glass coverslips (2.5 cm diameter) in 6-well plates at a density of 10^5 cells/well. Where indicated, coverslips were coated with fibronectin (0.1 mg/ml), fibrinogen (1 mg/ml), or poly-l-lysine (1 mg/ml), by allowing 100 ml of the indicated solution to air-dry on the coverslip. After coating, coverslips were washed with 1 M KCl and then with water before use.

Phagocytosis studies were performed by exposing cells to IgG-opsonized latex or zymosan particles at 37°C for the times indicated below. Particles had been opsonized by incubating with 1 mg/ml of human IgG for 1 h at 37°C, and where indicated, labeled by reacting with FITC (2 mg/ml in PBS, pH 8.0) for 1 h at 37°C. After repeated washing in PBS to remove unbound IgG or FITC, particles were suspended in Hepes-buffered RPMI and added to cells at a ratio of ~10 particles/cell. Where indicated, the cells were treated with cytochalasin D for 1 h at 37°C before the addition of particles.

For determination of Fcγ receptor clustering, cells were incubated with 1:200 anti–murine FcγRII/III receptor antibody followed by 1:500 of Cy3-conjugated donkey anti–rat antibody, each for 1 h at 4°C. Cross-linking was then allowed to occur by warming the cells to 37°C for 5 min. For determination of transferrin clustering and internalization, cells were incubated with Texas red–labeled human transferrin (25 μg/ml) for 1 h at 4°C to allow surface binding to occur. Internalization was induced by warming the cells to 37°C for 60 min.

Microinjection and Immunofluorescence Microscopy

For microinjection, cells were transferred to a Leiden coverslip holder and bathed in Hepes-buffered RPMI. Microinjection was performed using pipettes with tip diameter <1 μm pulled from filament-containing borosilicate capillaries with an inner diameter of 0.78 mm (Sutter Instruments, Novato, CA), using a Flaming/Brown model P87 micropipette puller (Sutter Instruments). C3 exotoxin (0.1 mg/μl) and the indicated fluorescent dye were dissolved in microinjection buffer. Solutions were injected into the cytoplasm of cells using a micromanipulator (model 5171; Eppendorf) and injector (model 5246; Eppendorf) under phase-contrast microscopy. A volume equivalent to ~10% of the total cell volume was injected. This was determined by injecting aqueous medium into oil containing 1-μm diameter latex beads and comparing the volume of the injected bubbles with the adjacent beads. After microinjection, cells were incubated in fresh medium at 37°C for the indicated periods.

For identification of microinjected cells during immunofluorescence experiments, cells were coinjected with Lucifer yellow (1 mg/ml). For F-actin staining, cells were fixed for 3 h with 4% paraformaldehyde in PBS at room temperature and washed in 100 mM glycine PBS for 10 min. The cells were then permeabilized in 0.1% Triton X-100 in PBS for 20 min at 22°C, washed in ice-cold PBS, and incubated with rhodamine-phalloidin (0.01 U/ml PBS) for 45 min at 22°C. For Fcγ receptor staining, fresh cells were incubated for 2 h at 4°C with a 1:200 dilution of anti-CD32/CD16 (FcγRII/III receptor) in 1% BSA-PBS. Coverslips were then washed three times in ice-cold PBS, and a 1:600 dilution of Cy3-labeled anti–rat antibody was added for 2 h at 4°C. Coverslips were then washed three times in ice-cold PBS and fixed in 4% paraformaldehyde for 3 h as above. For phosphotyrosine staining, cells were fixed and permeabilized as above, then blocked with 5% donkey serum in PBS for 1 h at room temperature. Coverslips were then incubated a 1:100 dilution of antiphosphotyrosine antibody and a 1:1,000 dilution of Cy3-labeled anti–mouse IgG as above. For MHC-I staining, cells were incu-

[1] *Abbreviations used in this paper:* $[Ca^{2+}]_i$, free cytosolic calcium; PAF, platelet-activating factor.

bated for 1 h at 4°C with undiluted hybridoma supernatant. Internalization was induced by incubating for 1 h at 37°C, then the cells were fixed, permeabilized, and blocked as above, and finally incubated with a 1:1,000 dilution of Cy3-labeled anti–mouse IgG.

After staining, cells were mounted using Slow Fade (Molecular Probes) and sealed with nail polish. Fluorescence was analyzed using (model TCS4D, Leica, Heidelberg, Germany) laser confocal microscope with a ×63 objective. Microinjected cells were identified by exciting the fluorescence of Lucifer yellow at 450 nm, while simultaneously analyzing the Cy3- or rhodamine-labeled molecule of interest by excitation at 540 nm. Composites of confocal images were assembled and labeled using Photoshop and Illustrator software (Adobe, Mountain View, CA). Quantification of immunofluorescence was performed using Adobe Photoshop. All experiments were performed at least four times. Representative confocal images are displayed where appropriate.

Single Cell Fluorescence Determinations

Determination of Phagocytosis. Phagocytosis was determined through the combined application of video microscopy and fluorescence ratio imaging. Identification of internalized particles was based on the low pH of the intraphagosomal milieu and its accessibility to ammonia, but not ammonium (see Results). Cells which had been exposed to opsonized, FITC-labeled particles for 1 h were washed with PBS and then placed in a thermostatted Leiden holder on the stage of a microscope (IM-35; Carl Zeiss, Inc., Thornwood, NY) equipped with a ×63, 1.4 numerical aperture oil-immersion objective. A filter wheel (Sutter Instruments) was used to alternately position the two excitation filters (500BP10 and 440BP10 nm) in front of a xenon lamp. To minimize dye bleaching and photodynamic damage, neutral density filters were used to reduce the intensity of the excitation light reaching the cells. The excitation light was directed to the cells via a 510 nm dichroic mirror. Data were recorded every 60 s by irradiating the cells for 250 ms at each of the excitation wavelengths. Image acquisition was controlled by the Metafluor software (Universal Imaging Corp., West Chester, PA), operating on a Pentium Dell computer (Dell Inc., Toronto, Ontario, Canada). The fluorescent light was directed onto a 535BP25 nm emission filter placed in front of a 512 frame-transfer cooled CCD camera (Princeton Research Instruments Inc., Princeton, NJ). The sample was continuously illuminated at 620 nm by placing a red filter in front of the transmitted incandescent source. By placing an additional dichroic mirror in the light path, the red light was directed to a video camera and optical disk recorder (TQ-2028F; Panasonic, Berkshire, UK), allowing continuous visualization of cell morphology and of the course of phagocytosis by Nomarski microscopy. Under these conditions, the rate of phagocytosis was comparable to that of nonilluminated controls. Calibration of the fluorescence ratio versus pH was performed in situ for each experiment by equilibrating the cells in isotonic K^+-rich medium buffered to varying pH values (between 6.0 and 7.45) in the presence of the K^+/H^+ ionophore nigericin (5 μM). Calibration curves were constructed by plotting the extracellular pH, which is assumed to be identical to the internal pH (18), against the corresponding fluorescence ratio.

To identify microinjected cells, C3 exotoxin (or vehicle buffer alone) was coinjected with fura-dextran (1 mg/ml). Injected cells were identified by illuminating the coverslips at 360 nm, the isosbestic excitation wavelength of fura, and directing the fluorescent light to the cells via a 410 nm dichroic mirror. There was no measurable contribution of fura-dextran emission when illuminating the samples under the conditions required for determination of FITC fluorescence (440 nm or 490 nm excitation, 510 nm dichroic mirror), ensuring that the microinjection marker did not interfere with the measurements of phagosomal pH.

Measurement of $[Ca^{2+}]_i$. Coverslips were mounted on the Leiden chamber as above and incubated with 10 mM of the acetoxymethyl ester form of fura-2 for 30 min at 37°C. The cells were then exposed to IgG-opsonized particles or to platelet-activating factor (PAF), and excited sequentially at 340 and 380 nm (500 ms each), capturing image pairs at 30-s intervals. The excitation light was directed to the cells via a 410 nm dichroic mirror and fluorescence emission was collected through a 540BP60 nm filter. Calibration of fluorescence ratio versus $[Ca^{2+}]_i$ was performed as described (19). For identification of microinjected cells during $[Ca^{2+}]_i$ determinations, cells were coinjected with FITC-dextran (1 mg/ml) and visualized by illumination at 440 nm, directed to the cells via a 510 nm dichroic mirror. The presence of the fluoresceinated dextran did not interfere with the $[Ca^{2+}]_i$ measurements.

Results

Assessment of Phagocytosis by J774 Macrophages and Fcγ Receptor–Transfected COS Cells. Microinjection of C3 exotoxin was the approach chosen to probe the role of Rho in phagocytosis. This required the implementation of single-cell assays of phagocytic function. Because morphological assessment of the association of particles with phagocytic cells is an ambiguous criterion, we developed a fluorescence ratio imaging approach to ensure the occurrence of phagosomal sealing. Intraphagosomal pH was measured using fluoresceinated, opsonized zymosan particles. Acidification of the milieu surrounding a particle was considered an initial indicator of phagosomal formation. As shown in Fig. 1, *A* and *B*, particles internalized by J774 cells can be readily identified by their acidic pH.

Because phagosome formation and acidification are sequential, separable events (20, 21), C3 exotoxin might conceivably impair the pH changes without preventing phagocytosis. We therefore assessed the formation of phagosomes by two other means. First, the pH of the opsonized particles was measured during exposure of the cells to NH_4Cl. Permeation of NH_3 (but not NH_4^+) across the plasma and phagosomal membranes, followed by protonation of the weak base induce an alkalinization of the particles within phagosomes, but not those adherent to the surface of the cells (e.g., Fig. 1 *C*). Because of the differential permeation of NH_3 and NH_4^+, an alkalinization should be apparent in particles secluded within phagosomes even if the latter fail to acidify. Second, abrupt changes in extracellular pH were imposed using impermeant acids (e.g., MES). This maneuver is expected to alter the pH of extracellular particles immediately, while having no acute effect on intraphagosomal particles (not shown). A combination of these three criteria, namely the basal pH and its sensitivity to added NH_4Cl and to extracellular acidification, was used routinely to identify bona fide intraphagosomal particles.

Fig. 1 also illustrates that the process of microinjection itself and the buffer used as a vehicle for C3 exotoxin had no discernible effects on the ability of the cells to engulf parti-

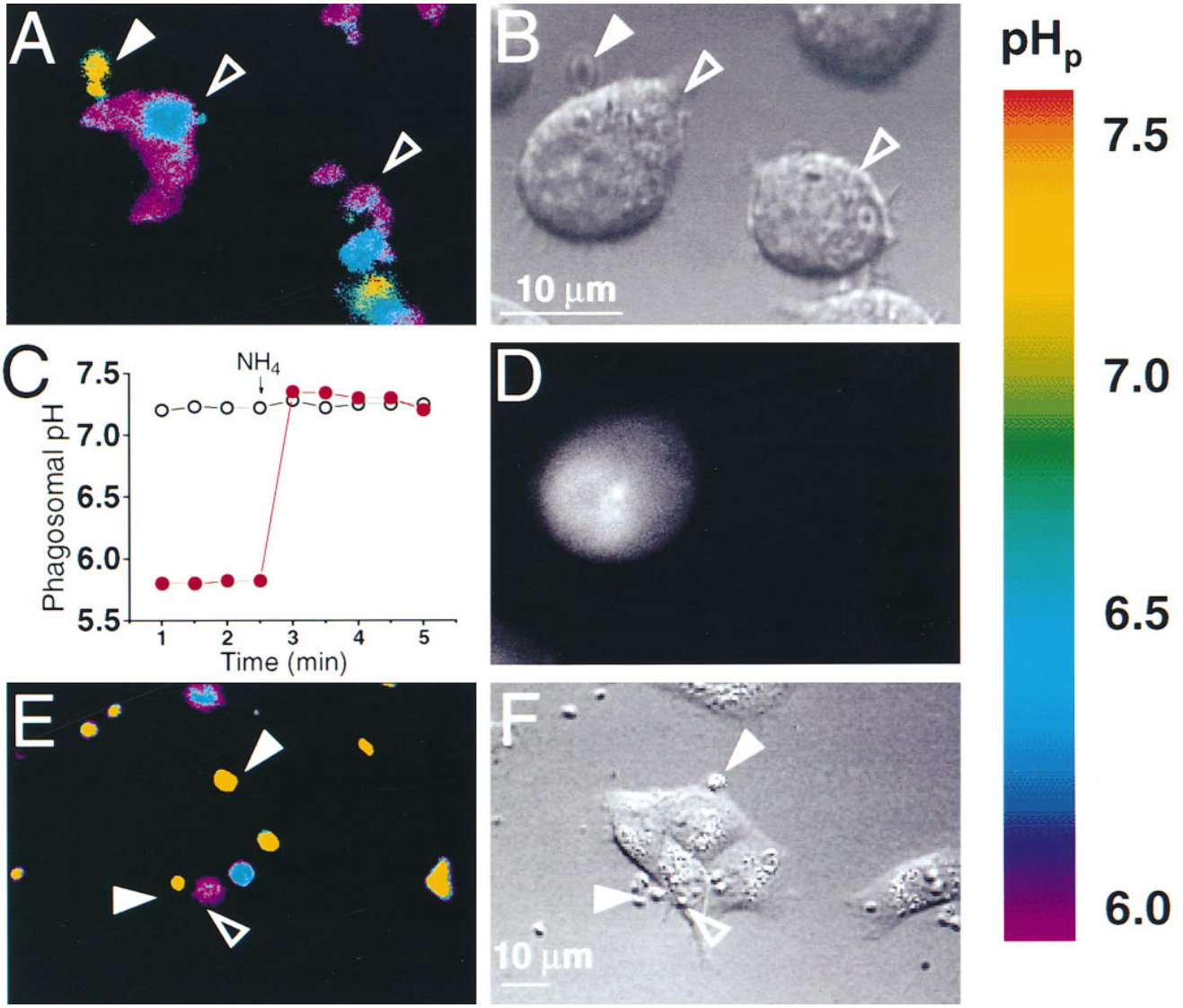

Figure 1. Determination of phagocytosis in J774 and FcγRIIA-transfected COS-1 cells. J774 macrophages (*A–D*) or FcγRIIA-transfected COS cells (*E* and *F*) were incubated with fluoresceinated, IgG-opsonized zymosan particles, some of which became internalized. (*A*) The fluorescence emitted by the particles was measured with alternating excitation at 440 nm and 490 nm, and the fluorescence ratio was used to estimate the pH at the particle surface. A pseudocolor image is shown in *A*, corresponding to the pH scale shown to the right. Extracellular particles (*solid arrowheads*) display higher pH values than internalized particles (*open arrowheads*). (*B*) The cells in *A* as visualized using differential interference contrast (Nomarski) optics. (*C*) Time course of pH changes observed in an alkaline (likely extracellular; *open white circles*) and an acidic (likely intraphagosomal; *solid red circles*) particle. Where indicated, 50 mM NH_4Cl was added to the medium, producing alkalinization of internalized particles. (*D*) The left hand cell in *A* and *B* underwent control microinjection with the injection marker, fura-dextran, dissolved in injection buffer alone. The fluorescence emission of fura (excitation: 360 nm; emission: 535 nm) is illustrated. (*E*) Pseudocolor image of the fluorescence ratio of IgG-opsonized zymosan particles incubated with FcγRIIA-transfected COS-1 cells. Extracellular particles (*solid arrowheads*) display higher pH values than internalized particles (*open arrowheads*). (*F*) The cells in *A* as visualized using differential interference contrast optics. Representative of at least five separate experiments of each type.

cles and to acidify the phagosomal lumen. As illustrated in Fig. 1 *D*, coinjection of fura-dextran enabled us to identify microinjected cells, without interfering with the pH determinations. Microinjected (fura-dextran–containing) cells retained normal morphology and, more importantly, were able to internalize and acidify particles. The percentage of phagocytosis-competent cells was similar in uninjected versus injected cells (53 ± 5 and 51 ± 3%, respectively, means ± SE of three experiments, each with at least 50 control and 50 experimental cells). These findings validated the use of microinjection to assess the role of Rho in phagocytosis and cellular morphology.

A variety of receptors, using different signal transduction pathways, can promote phagocytosis. To facilitate the interpretation of our experiments, the particles used in Fig. 1, *A–D*, had been pretreated with a single opsonin, IgG, to promote activation of phagocytosis via a single family of receptors, namely Fcγ receptors. Nevertheless, the receptor

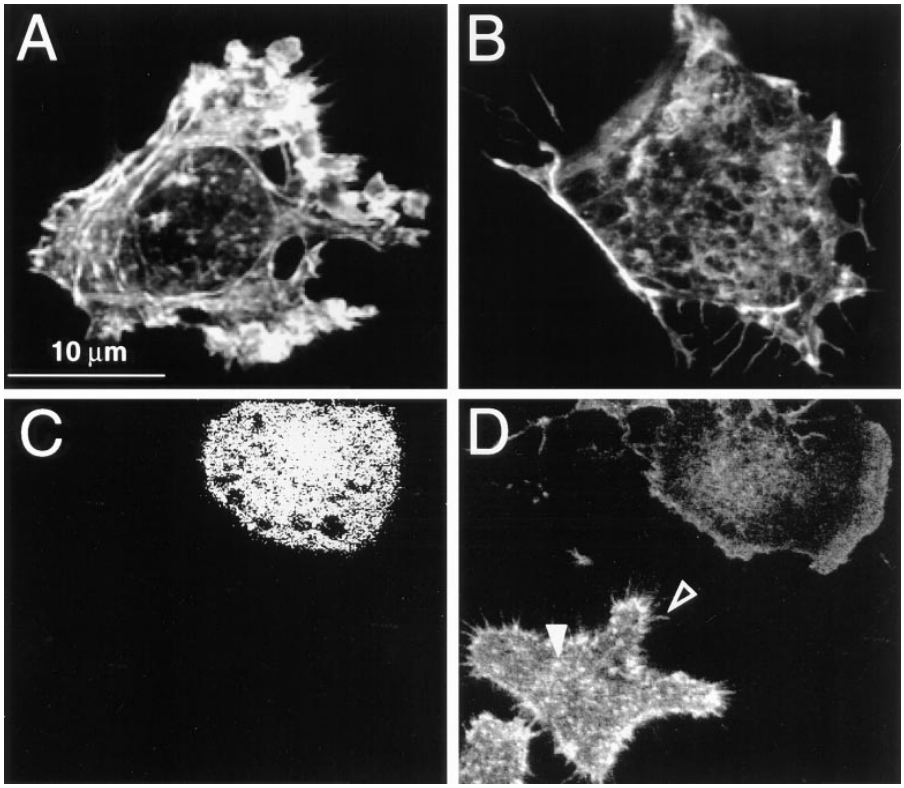

Figure 2. The effect of microinjected C3 exotoxin on the actin cytoskeleton of FcγRIIA-transfected COS and J774 cells. (*A*) FcγRIIA-transfected COS cells were mock-injected with the fluorescent dye Lucifer yellow dissolved in injection buffer alone, fixed, and stained with rhodamine phalloidin to visualize F-actin. Note the presence of stress fibers and actin accumulation at adhesion plaques. (*B*) FcγRIIA-transfected COS cells were injected with C3 exotoxin 60 min before fixation and staining with rhodamine phalloidin. Note the disappearance of stress fibers and focal adhesions and the persistence of F-actin along membrane ruffles. (*C*) Lucifer yellow emission of J774 cells, identifying the top cell as having been injected with C3 exotoxin. (*D*) Rhodamine-phalloidin staining of the cells shown in *C*. Note the decrease in F-actin content, and the absence of filopodia (*open arrowhead*) and focal complexes (*solid arrowhead*) in the C3-injected cell (*top right*) compared to the uninjected (*bottom left*) cells. Representative of eight separate experiments.

responsible for internalization is difficult to define unambiguously, given the multiplicity of phagocytic receptors on the surface of macrophages. To circumvent this complexity we also analyzed COS cells that had been heterologously transfected with FcγRIIA receptors. As described earlier (17), transfection of FcγRIIA receptors confers phagocytic properties to these cells, which are otherwise unable to perform phagocytosis. As illustrated in Fig. 1, *E* and *F*, phagocytosis of opsonized zymosan by the COS transfectants was also discernible by measuring the pH using ratio imaging, and was unaltered by microinjection of control solution (not shown). These results confirm that the transfected COS cells display a phenotype similar to that of professional phagocytes (17), and thus provide a model for the study of the effects of Rho on Fcγ receptor–mediated phagocytosis.

Effect of C3 Exotoxin on the Actin Cytoskeleton of COS-2A and J774 Cells. We next sought to define the conditions required for inactivation of Rho in phagocytic cells. In fibroblasts, ADP-ribosylation of Rho by microinjection of C3 exotoxin has been demonstrated to disrupt preformed stress fibers and focal adhesions (22). Because J774 macrophages lack well defined stress fibers and adhesion plaques, we first tested the effectiveness of the exotoxin on the FcγRIIA receptor–transfected cells. As shown by the phalloidin staining pattern of F-actin shown in Fig. 2 *A*, the transfectants display clearly identifiable focal adhesions and stress fibers. Phalloidin staining was also detectable in the ruffled borders of lamellipodia. Microinjection of the cells with vehicle containing only Lucifer yellow, the fixable marker used to identify the injected cells, had no discernible effect on the distribution of F-actin. By contrast, microinjection of the transfectants with C3 exotoxin induced profound alterations in the F-actin pattern (Fig. 2 *B*). The stress fibers and adhesion plaques were largely eliminated, resulting in a sizable decrease in the overall amount of bound phalloidin. In C3-treated cells F-actin was mainly detectable along the borders.

The distribution of F-actin in control and C3-injected J774 cells is compared in Fig. 2 *D*. The C3-treated cell is identifiable in Fig. 2 *C* by the emission of Lucifer yellow, the injection marker. The total phalloidin staining of untreated cells was considerably greater than that of C3-injected cells. F-actin accumulated in control cells along the cell borders and in fine filopodia (*open arrowhead* in Fig. 2 *D*), as well as in focal complexes throughout the adherent membrane (*solid arrowhead*). Rho seemed to be essential for the maintenance of filopodia and focal complexes in J774 cells, since these structures were eliminated or greatly reduced by C3 exotoxin (Fig. 2 *D*; representative of three experiments, each with at least 50 injected cells). As in the COS cells, F-actin persisted mainly along the borders of C3-treated J774 cells.

Effects of Rho on Cell Morphology and Phagocytosis. Having established the functional capacity of microinjected C3 on J774 and Fcγ receptor–transfected COS cells, we next investigated the effects of the exotoxin on cell morphology and phagocytosis. To this end, we used a unique micro-

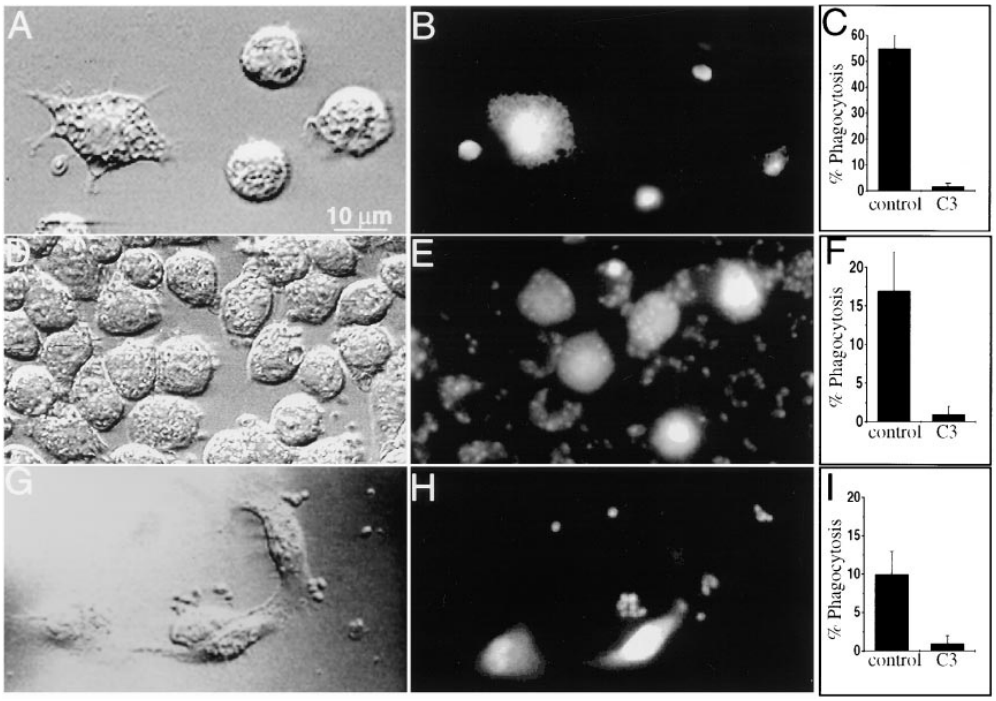

Figure 3. The effect of Rho inhibition on cell morphology and phagocytosis. (*A–C*) J774 cells were plated on glass and some were injected with C3 exotoxin in a solution containing fura-dextran as a marker. The cells were then incubated with fluoresceinated, opsonized zymosan. (*A*) Differential interference contrast micrograph. Note the morphological alterations of the left hand, injected cell. (*B*) Fluorescence emission of the cells shown in *A* (excitation 360 nm; emission 510 nm). The emission of fura-dextran, demonstrating that only the left hand cell was injected. The emission of fluorescein, which can be seen despite the low excitation wavelength, reveals the labeled zymosan particles. (*C*) Effect of C3 exotoxin on phagocytosis by cells plated on glass, determined as described in Materials and Methods. Data are means ± SE of 175 control and 160 C3-injected cells ($P < 0.05$.). (*D–F*) J774 cells were plated on fibronectin and some were injected with C3 exotoxin as above. The cells were then incubated with fluoresceinated, opsonized zymosan. (*D*) Differential interference contrast micrograph. (*E*) Fluorescence emission of the cells shown in *D*. (*F*) Effect of C3 exotoxin on phagocytosis on fibronectin. Data are means ± SE of 150 control and 74 C3-injected cells ($P < 0.05$). (*G–I*) FcγRIIA receptor–transfected COS cells were plated on glass coverslips and some were injected with C3 exotoxin as above. The cells were then incubated with fluoresceinated, opsonized zymosan. (*G*) Differential interference contrast micrograph. (*H*) Fluorescence emission of the cells shown in *G*. (*I*) Effect of C3 exotoxin on phagocytosis by transfected COS cells. Data are means ± SE of 165 control and 75 C3-injected cells ($P < 0.05$). Images are represented of five separate experiments.

scopic configuration which enabled us to simultaneously monitor cell shape, using differential interference contrast (Nomarski) optics, and phagosomal pH by fluorescence ratio imaging, as described above. Moreover, by modifying the excitation wavelength, microinjected cells could be identified by the emission of the injection marker, fura-dextran (Fig. 3).

When allowed to adhere to glass coverslips, uninjected (or mock-injected) J774 cells appeared roughly spherical (Fig. 3, *A* and *B*, *right hand cells*). By contrast, C3-injected cells were considerably flatter, spreading over a greater area of the substratum (Fig. 3, *A* and *B*, *left hand cell*). Extensions were often seen protruding from the cells, as if their adherence to the surface had increased. In addition, C3-injected cells exhibited increased accumulation of large vacuolar structures (Fig. 3 *A*), with features resembling macropinosomes (23). These changes were evident within 20 min of injection of C3 exoenzyme.

Importantly, the ADP-ribosylation of Rho resulted in the near total loss of the ability of J774 cells to engulf IgG-opsonized zymosan particles (Fig. 3 *C*). Whereas 53 ± 5% of control cells internalized at least one zymosan particle, only 2 ± 1% of the C3-injected cells were phagocytosis competent (means ± SE of seven experiments, each with at least 50 cells/group). The impairment of phagocytosis in the C3-treated cells may have resulted from their increased adherence to the substratum, perhaps precluding the interaction of particles with Fcγ receptors. To examine this possibility, we sought to preserve the native morphology of the cells after microinjection of C3 exoenzyme. This was attempted by varying the nature of the substratum used for cell plating. We found, empirically, that otherwise untreated cells adhered more effectively to fibronectin than to glass, resulting in higher cell densities after plating comparable numbers of cells (compare Fig. 3, *A* and *D*). More importantly, cells plated on fibronectin and injected with C3 exotoxin retained a morphology which was indistinguishable from that of control cells (Fig. 3 *D* and *E*). Phagocytosis was somewhat lower in control cells plated on fibronectin, compared to cells on glass (Fig. 3 *C* vs. *F*). Nevertheless, the efficiency of phagocytosis was sufficiently high to allow the assessment of the role of Rho in the process. As shown in Fig. 3 *F*, phagocytosis was virtually eliminated by injection of fibronectin-plated cells with C3 exotoxin (controls, 17 ± 5%; C3-injected, 1 ± 1%; means ± SE of five experiments with at least 50 cells/group). Similar inhibitory effects of the exotoxin were obtained in cells plated on fibrinogen, collagen, or poly-l-lysine (data not shown). Together these data indicate that Rho is essential for phagocytosis in macrophages and that the inhibitory action of C3 is independent of its effects on cellular morphology.

This conclusion was supported by observations made in FcγRIIA receptor–transfected COS cells. Unlike J774 cells, COS cells plated on glass did not undergo detectable

morphological changes when injected with C3 exotoxin (Fig. 3, *G* and *H*). Nevertheless, phagocytosis was markedly decreased in these cells compared to noninjected controls (Fig. 3 *I*). In three separate experiments, 12 ± 3% of the control cells internalized IgG-opsonized zymosan, compared to only 2 ± 1% of the C3-injected cells (mean ± SE of at least 25 cells/group in each experiment). In conjunction with the above data, these findings indicate that Rho is essential for Fcγ receptor-mediated phagocytosis.

The Effect of Rho on Fcγ Receptor–induced Calcium Signaling. An increase in $[Ca^{2+}]_i$ mediated by activation of phospholipase C and release of Ca^{2+} from intracellular pools, is one of the earliest consequences of Fcγ receptor ligation (7, 24). This $[Ca^{2+}]_i$ transient is not essential for phagocytosis (25–27), suggesting the existence of parallel signaling pathways. We questioned whether Rho was required specifically for phagocytosis or whether other Fcγ receptor–mediated signaling cascades also involved this GTP-binding protein. We therefore evaluated the effects of C3 exoenzyme on the $[Ca^{2+}]_i$ transients evoked by IgG-opsonized particles, using fura-2. Single cell ratio imaging was required for these experiments due to the transient nature of the $[Ca^{2+}]_i$ rises which occur in response to particulate stimuli (28). Representative tracings from eight individual cells are illustrated in Fig. 4. Control cells respond to the addition of zymosan with single or repetitive $[Ca^{2+}]_i$ transients (Fig. 4, *A–C*). Comparable $[Ca^{2+}]_i$ changes were not detected in C3-treated cells (Fig. 4, *D–F*), implying that Rho is required for phospholipase C activation. The inhibitory effects of the exotoxin are not due to a general detrimental effect on the cells. This is suggested by two observations. First, the resting $[Ca^{2+}]_i$ was comparable in C3-injected and untreated cells. Second, both the injected and the control cells responded similarly to the addition of PAF, an agonist that activates serpentine receptors coupled to heterotrimeric G proteins (see Fig. 4). These results demonstrate that Rho is essential for multiple aspects of Fcγ receptor signaling.

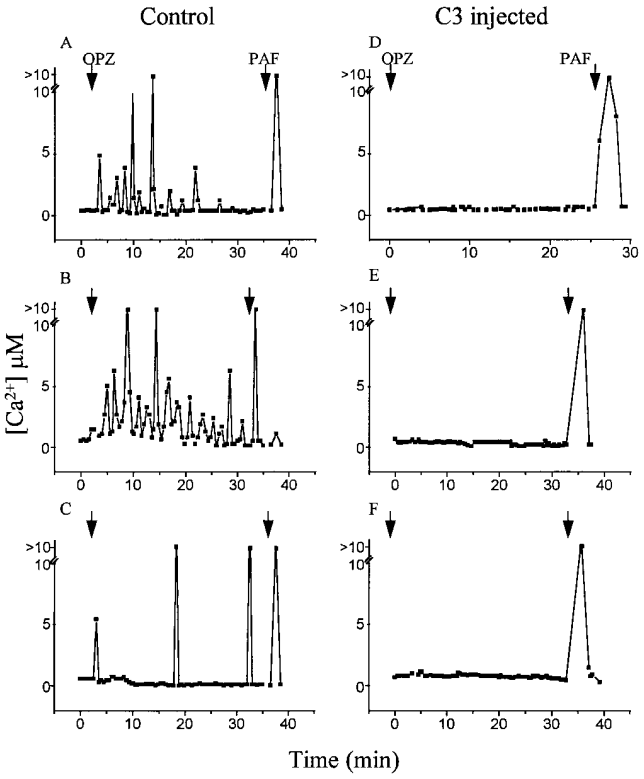

Figure 4. Effect of Rho on Fcγ receptor–mediated increases in $[Ca^{2+}]_i$. J774 cells, some of which had been microinjected with C3 exotoxin 1 h before, were loaded with fura-2. The concentration of $[Ca^{2+}]_i$ was measured by ratio imaging as described in Materials and Methods. Where indicated, the cells were exposed to opsonized zymosan (*OPZ*) or to PAF (1 μM). Injected cells were identified by the fluorescence of the injection marker, fluorescein dextran. The changes in $[Ca^{2+}]_i$ from eight separate cells are shown. Control cells : *A–C*. C3-injected cells: *D–F*. Uninjected cells exhibited transient, asynchronous rises in $[Ca^{2+}]_i$ in response to opsonized zymosan and a synchronous rise in response to PAF. By contrast, C3-injected cells did not exhibit changes in $[Ca^{2+}]_i$ in response to zymosan, yet responded to PAF. Representative of five separate experiments with at least eight cells/group.

Role of Rho in Phagocytic Cup Formation and in Phosphotyrosine Accumulation. Clustering of the Fcγ receptors in macrophages upon interaction with IgG-opsonized particles leads to the accumulation of F-actin and tyrosine kinases around nascent phagocytic cups (4, 5, 29). Both of these events have been claimed to be required for induction of the $[Ca^{2+}]_i$ response to phagocytes to opsonized particles (30, 31). It was therefore of interest to define whether tyrosine phosphorylation and actin polymerization, which precede the completion of phagocytosis, are also dependent on Rho, or whether the GTP-binding protein lies downstream of these events. To study actin assembly around phagocytic cups, C3-injected and uninjected J774 cells were incubated for 30 min with IgG-opsonized particles, rapidly fixed, and stained with rhodamine-phalloidin. This time point was determined to be optimal for detection of nascent phagocytic cups. Adhesion of the fluoresceinated particles and the distribution of F-actin were determined using dual wavelength confocal microscopy. As before, injected cells were identified by coinjection of Lucifer yellow. The fluorescence emission of the zymosan particles and of Lucifer yellow, indicative of C3-injected cells, is shown in Fig. 5 *A*, while the corresponding F-actin staining is shown in Fig. 5 *B*. Notice that a greater number of particles adhered to untreated cells compared to C3-injected cells (untreated, 15 ± 5 adherent particles/cell; C3 injected, 3 ± 1 particles/cell; mean of four experiments with at least 50 cells each; $P < 0.05$). As described earlier (4), during the early stages of phagocytosis F-actin accumulated in cuplike structures underneath the region of the membrane adherent to particles. Such F-actin cups were totally absent from C3-injected cells (Fig. 5 *B*). These data demonstrate that Rho plays important roles in mediating particle adherence as well as the accumulation of F-actin around adherent particles.

The effects of Rho on phosphotyrosine accumulation at phagocytic cups are illustrated in Fig. 5, *C–E*. J774 cells were incubated with opsonized latex beads as above and the accumulation of tyrosine phosphorylated proteins was

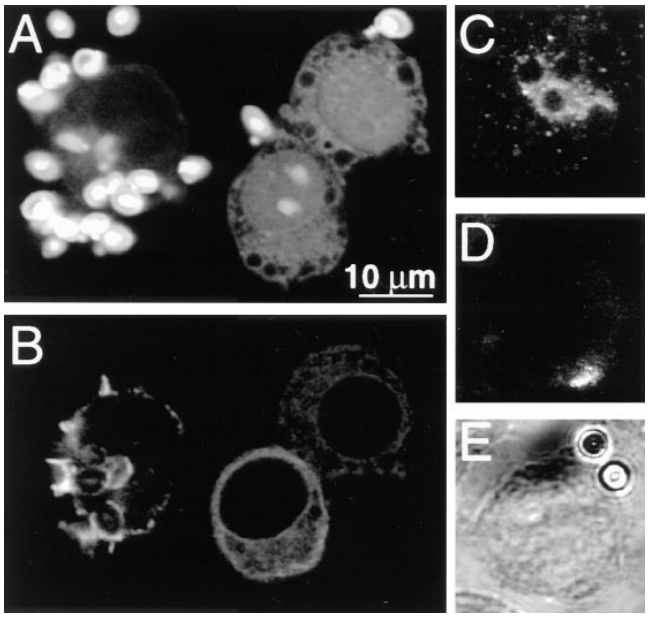

Figure 5. Effect of C3 microinjection on the accumulation of F-actin and phosphotyrosine at nascent phagocytic cups. Fluoresceinated, opsonized zymosan particles were added for 30 min to J774 cells, some of which had been injected with C3 exotoxin and Lucifer yellow 1 h before. (*A–D*) Confocal fluorescence images. (*A*) Green fluorescence emission showing the particles and identifying the injected cells. Note that the two right hand cells were injected, and bound fewer particles compared with the uninjected cell (*left hand*) (*B*) Red fluorescence illustrating the distribution of F-actin, stained with rhodamine-phalloidin. Note the F-actin cups in uninjected cells but not in C3-injected cells. (*C*) Immunostaining of a control cell with antiphosphotyrosine antibody. The accumulation of phosphotyrosine at phagocytic cups is illustrated. (*D*) Antiphosphotyrosine staining of a C3-injected cell, identified by the emission of Lucifer yellow (not shown). Note the absence of phosphotyrosine accumulation at sites where latex particles adhered (see *E*). (*E*) Differential interference contrast micrograph of the cell in *D*. Images are representative of five experiments of at least 20 cells/experiment.

determined using confocal immunomicroscopy. Latex particles were used for these studies to circumvent the nonspecific binding of antibodies inherent to zymosan. In control cells, phosphotyrosine was found to accumulate around nascent phagosomes, as described earlier (5). However, such accumulations were not found in cells treated with C3 exotoxin, even when beads were found adhered to their surface (Fig. 5 *D* and *E*). These results imply that functional Rho is required for the accumulation of phosphotyrosine at nascent phagosomes and may therefore be an essential step in the signaling cascade leading to phagocytosis.

Effect of C3 Exotoxin on the Surface Expression of Fcγ Receptors The above data indicated that inactivation of Rho impaired the signaling normally observed upon Fcγ receptor ligation. In principle, these observations may result from a decrease in the abundance of Fcγ receptors expressed on the cell surface. In support of this interpretation is the observation that fewer IgG-opsonized particles adhered to C3-injected cells compared to their noninjected counterparts (Fig. 5 *A*). To assess this possibility, we compared the density of Fcγ receptors in C3-injected and in untreated J774 cells, using immunofluorescence confocal microscopy (Fig. 6). To ensure the accurate determination of the total number of surface receptors while accounting for the changes in morphology which occurred upon C3 microinjection, three-dimensional reconstructions were generated by integrating serial confocal scans in the horizontal (x vs. y) plane. A representative field and collated results from 20 cells from four experiments are shown in Fig. 6, *B* and *C*, respectively. Fig. 6 *A* illustrates the fluorescence of Lucifer yellow, the injection marker. There were no significant differences in the density of FcγRII/III receptor expression in C3-injected compared to untreated cells (Fig. 6, *B* and *C*). These data suggest that Rho is not required for the maintenance of Fcγ receptors at the cell surface.

Effect of C3 Exotoxin on Fcγ Receptor Clustering. Upon interaction with ligand, receptors are induced to cluster within the cell membrane (6). The aggregation of Fcγ receptors, which have comparatively low affinity, is essential for stabilization of their interaction with multivalent ligands (32, 33). In addition, receptor cross-linking leads to the generation of the intracellular signals required to trigger phagocytosis (5, 29). We therefore investigated the possibility that Rho was required for the displacement of receptors in the plane of the membrane and/or to stabilize their association. To examine the role of Rho on receptor clustering, control and C3-injected J774 cells were treated with soluble anti-Fcγ receptor antibody, followed by a secondary antibody to induce cross-linking and to visualize the cells by fluorescence. Receptor distribution was then examined by

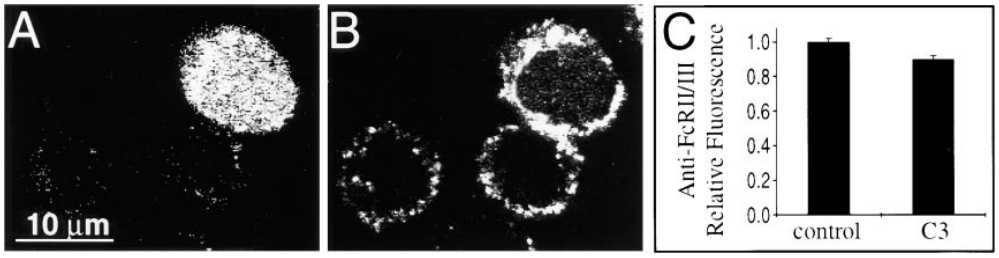

Figure 6. Quantification of Fcγ receptors on the surface of control and C3-injected cells. J774 cells were injected with C3 exotoxin and the fluorescent dye (Lucifer yellow) 1 h before the determination of Fcγ receptor expression using anti-FcγII/III receptor antibodies and confocal microscopy. (*A*) Lucifer yellow fluorescence, demonstrating that the upper right hand cell had been injected. (*B*) Corresponding confocal micrograph illustrating the abundance and distribution of Fcγ receptors. (*C*) Quantification of relative fluorescence intensity of cells stained with anti-FcγII/III receptor antibodies, as in *B*. Data are means ± SE of 75 control and 53 C3-treated cells.

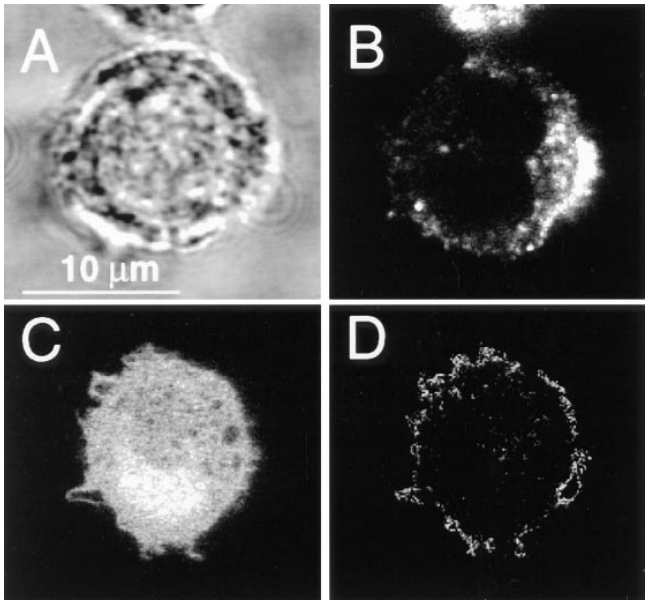

Figure 7. Effect of Rho on Fcγ receptor clustering. (*A*) Differential interference contrast image of a J774 cell which had been exposed to anti-Fcγ receptor antibody and to secondary antibody in the cold, followed by incubation for 5 min at 37°C to induce cross-linking of Fcγ receptors. (*B*) Confocal micrograph illustrating the Fcγ receptor distribution of the cell in *A*. Note the polar distribution of receptors. (*C*) Lucifer yellow emission identifying a cell which had been injected with C3 exotoxin 1 h before receptor cross-linking, which was performed as in *A*. (*D*) Confocal micrograph illustrating the Fcγ receptor distribution of the cell in *C*. Note that receptor clustering did not occur (compare *B* and *D*). Representative of five separate experiments of at least 20 cells/experiment.

confocal microscopy. 5 min after induction of cross-linking, control cells demonstrated clustering of receptors at discrete areas of the plasma membrane (Fig. 7, *A* and *B*). In contrast, receptor capping was inhibited in C3-injected cells, which displayed diffuse fluorescence throughout the surface. These findings suggest that Rho plays an essential role in Fcγ receptor clustering and suggests a mechanism whereby this GTP-binding protein regulates the process of phagocytosis.

These observations raised the possibility that, by altering the cytoarchitecture, C3 exotoxin might affect not only the clustering of Fcγ receptors, but the mobility of surface receptors in general. To investigate this possibility, we examined the effect of the toxin on the uptake of transferrin by J774 cells. The uptake of transferrin depends upon the lateral diffusion and clustering of its receptors at clathrin-coated pits, which is immediately followed by internalization via clathrin-coated vesicles (34). This process is illustrated in Fig. 8. To demonstrate binding to its surface receptors, J774 cells were incubated at 4°C with Texas red–labeled transferrin, and examined by confocal microscopy. At this temperature, lateral diffusion and internalization are precluded and the label is found exclusively at the cell surface (Fig. 8, *A* and *B*). To effect internalization, the cells were then warmed to 37°C for 1 h, resulting in a marked redistribution of transferrin into a punctate, vesicular pattern (Fig. 8 *C*), consistent with the reported localization of transferrin receptors to a recycling endosomal compartment (35, 36). As shown in Fig. 8, *D* and *E*, neither the binding nor the internalization of transferrin was affected by earlier injection of the cells with C3 exotoxin. These observations imply that Rho is not required for the clustering of transferrin receptors at clathrin-coated pits or for their subsequent endocytosis, and are in good agreement with the findings of Lamaze et al. (37). C3 injection was also without effect on the internalization of MHC-I, measured using a monoclonal antibody (not illustrated). Together, these findings indicate that Rho is not essential for the lateral mobility, clustering, and internalization of all surface receptors and that the effects of C3 on Fcγ receptors are specific.

Discussion

The role of Rho in phagocytosis was explored by microinjection of C3 exotoxin from *C. botulinum*. Under conditions similar to the ones we used, C3 exotoxin has been shown to impair Rho very specifically (38, 39), though other possible effects of the toxin cannot be completely discounted. The activity of the exotoxin was demonstrated by the drastic reduction in the stress fiber and focal adhesion content of injected COS cells. In J774 macrophages, which lack well-defined stress fibers and adhesions, inactivation of Rho resulted in disappearance of focal complexes and retraction of filopodial extensions. In both cell types the overall content of F-actin was markedly decreased, resembling results obtained with most other cell types (40, 41), although exceptions have been noted (22).

Microinjection of cells plated on glass induced several morphological alterations. First, the cells were markedly flatter with extensions, suggesting that adherence was enhanced (Fig. 3). Analogous results have been reported in U937 and in neuronal cells (42, 43). However, these changes are not a feature of all cells nor are they common to all substrata. For example, in this study, spreading was stimulated only on glass, but not on protein- or poly-l-lysine–coated coverslips. By contrast, C3-treated U937 cells flattened onto fibronectin, but not collagen- or serum-coated surfaces (44). The mechanism underlying increased adherence remains undefined, but is not due to changes in the number of receptors (44). C3-injected J774 cells also exhibited the accumulation of large cytoplasmic vacuoles (Fig. 3 *A*). These may reflect an increased capacity of the cells to perform endocytosis, which is known to be negatively regulated by active Rho (37). Jointly, these observations indicate that Rho plays a critical role in maintaining the cytoskeletal architecture of macrophages.

The most striking consequence of inhibiting Rho detected in this study was the impairment in phagocytosis. This inhibition was not a consequence of the altered cell morphology induced by C3, since it was also observed in cells plated on matrices where spreading did not occur. Inhibition of phagocytosis was paralleled by reduced adherence of the IgG-opsonized particles to the surface of the cells. The latter observation suggested that C3-treated cells are unable to undergo clustering of Fcγ receptors, which

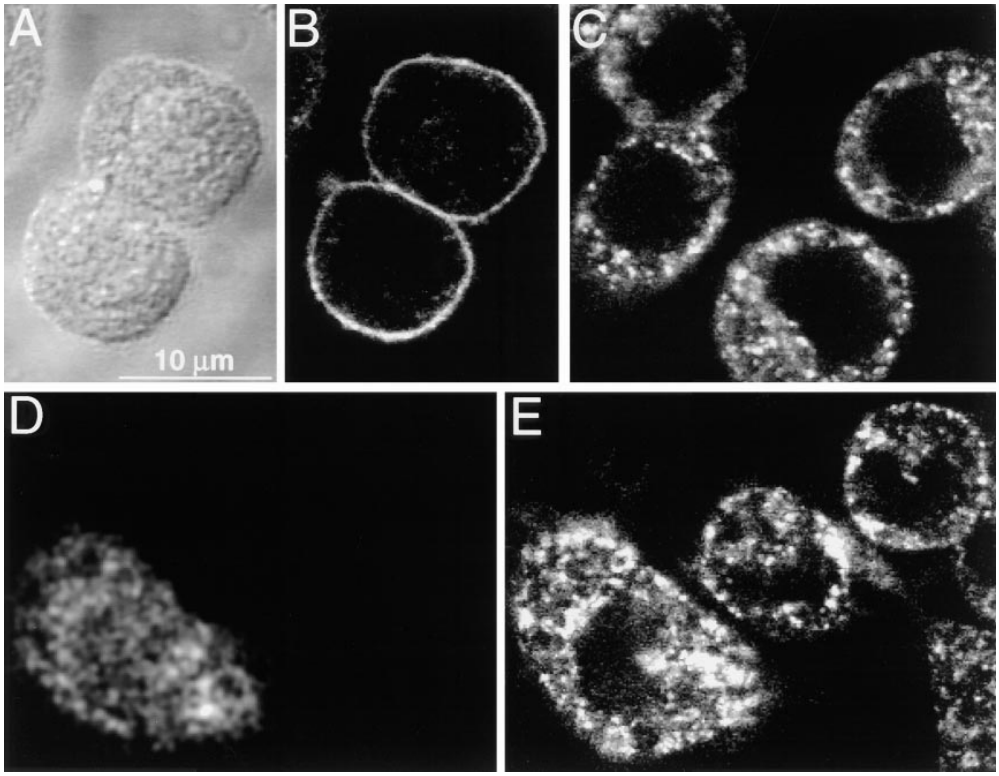

Figure 8. Transferrin internalization in J774 cells: effect of C3 exotoxin. (*A*) Differential interference contrast image of J774 cells which had been exposed to Texas red–labeled transferrin for 1 h at 4°C. (*B*) The cells in *A* were analyzed by confocal fluorescence microscopy to detect the distribution of transferrin. (*C*) Cells were initially incubated with Texas red–labeled transferrin as in *A* and then warmed to 37°C for another hour to promote receptor internalization. A typical confocal micrograph is illustrated. (*D* and *E*) Selected cells were injected with C3 exotoxin and Lucifer yellow (as a marker of microinjection) and the whole cell population was then allowed to bind and internalize Texas red–labeled transferrin as in *C*. (*D*) Lucifer yellow emission identifying a cell which had been injected with C3 exotoxin ~1 h before exposure to transferrin. (*E*) Confocal micrograph illustrating the distribution of transferrin in the same cells as shown in *D*. Note that internalization occurred similarly in both injected cells (left hand cell in *E*) and noninjected cells. Representative of three separate experiments, with at least 25 injected cells/experiment.

may be required to stabilize their interaction with multivalent ligands. In this context, it is noteworthy that Rho is believed to be essential to stabilize receptor (integrin) complexes within adhesion plaques (45). Clustering of integrins, which occurs upon contact of cells with the extracellular matrix (46), results in the assembly of multimolecular complexes which link the integrins to the actin cytoskeleton through adaptors including α-actinin, vinculin, and talin (47). The formation of these complexes requires intact Rho (45) and is associated with recruitment of this GTP-binding protein to the cell surface (48).

These analogies prompted us to evaluate the role of Rho in Fcγ receptor clustering. Our results indicate that while the number of receptors on the surface is unaffected by C3 exotoxin their ability to cap upon cross-linking was impaired. Failure of the Fcγ receptors to cluster most likely explains their inability to trigger normal tyrosine phosphorylation, calcium release, and actin cup formation, as well as their reduced adherence of opsonized particles.

Clustering of a variety of cell surface receptors on the surface of leukocytes and the adhesivity of the cells to the matrix or to phagocytic particles are known to involve F-actin, inasmuch as they are inhibited by cytochalasins (49, 50). It is possible therefore that depolymerization of F-actin by C3 exoenzyme mediates the observed inability of the receptors to cluster. In a similar fashion, capping of Fcγ receptors in J774 cells was inhibited in cytochalasin D–treated cells (not shown). Importantly, C3 exotoxin was found to be without effect on the clustering and internalization of transferrin receptors (Fig. 8) and MHC-1 (data not shown), which are thought to be actin-independent processes. This excludes a generalized, nonselective effect of the toxin on receptor mobility within the plasma membrane, and implicates Rho specifically in the cascade of events leading to the F-actin rearrangements required for clustering of the Fcγ receptors. However, it is also possible that Rho may stabilize receptor complexes by means other than actin assembly, since in fibroblasts adhesion plaques persist in the presence of cytochalasin in a Rho-dependent manner (22). Hence, this GTP-binding protein may play additional signal transducing roles leading to the formation or stabilization of receptor clusters. Clearly, Rho could also play additional roles in signaling downstream events in the phagocytic sequence.

In summary, we have identified the small GTPase Rho as a critical regulator of Fcγ receptor–mediated phagocytosis in cultured macrophages. Rho was found to exert its effects, at least in part, at the level of Fcγ receptor clustering.

By regulating this most proximal step, Rho was found to be essential for F-actin rearrangement, phosphotyrosine accumulation, and increases in intracellular Ca^{2+}, processes that ultimately lead to the phagocytosis and killing of microbial pathogens. It is important to stress that these conclusions should at present be confined to transformed cell lines. Generalization of these notions awaits direct experiments in native macrophages.

This research was funded by operating grants awarded to S. Grinstein and O.D. Rotstein by the Medical Research Council of Canada. D.J. Hackam is the recipient of a Medical Research Council of Canada Fellowship and an Ethicon-Society of University Surgeons Surgical Research Award. S. Grinstein is an International Scholar of the Howard Hughes Medical Institute.

Address correspondence to Dr. Sergio Grinstein, Division of Cell Biology, Hospital for Sick Children, 555 University Avenue, Toronto, Ontario, Canada M5G 1X8. Phone: 416-813-5727: FAX: 416-813-5028; E-mail: sga@sickkids.on.ca

Received for publication 9 May 1997 and in revised form 8 July 1997.

References

1. Greenberg S., and S.C. Silverstein. 1993. Phagocytosis. *In* Fundamental Immunology. W.E. Paul, editor. Raven Press, Inc., New York. 941–964.
2. Swenson, J.A., and S.C. Baer. 1995. Phagocytosis by zippers and triggers. *Trends. Cell Biol.* 5:89–94.
3. Greenberg, S., P. Chang, D. Wang, R. Xavier, and S. Seed. 1996. Clustered syk tyrosine kinase domains trigger phagocytosis. *Proc. Natl. Acad. Sci. USA.* 93:1103–1107.
4. Cox, D., P. Chang, T. Kurosaki, and S. Greenberg. 1996. Syk tyrosine kinase is required for immunoreceptor tyrosine activation motif-dependent actin assembly. *J. Biol. Chem.* 271:16597–16602.
5. Greenberg, S., P. Chang, and S.C. Silverstein. 1993. Tyrosine phosphorylation is required for Fc receptor mediated phagocytosis in mouse macrophages. *J. Exp. Med.* 177:529–534.
6. Indik, Z.K., J. Park, S. Hunter, and A.D. Schreiber. 1995. The molecular dissection of Fc receptor mediated phagocytosis. *Blood.* 86:4389–4396.
7. Rosales, C., and E. Brown. 1992. Signal transduction by neutrophil immunoglobulin G Fc receptors: dissociation of intracytoplasmic calcium concentration rise from inositol 1,4,5-triphosphate. *J. Biol. Chem.* 267:5265–5271.
8. Ridley, A.J., and A. Hall. 1992. The small GTP-binding protein rho regulates the assembly of focal adhesions and stress fibers in response to growth factors. *Cell.* 70:389–399.
9. Coso, O.A., M. Chiariello, J.-C. Yu, H. Teramoto, P. Crespo, N. Xu, T. Miki, and J.S. Gutkind. 1995. The small GTP-binding proteins Rac1 and CDC42 regulate the activity of the JNK/SAPK signaling pathway. *Cell.* 81:1137–1146.
10. Hill, C.S., J. Wynne, and R. Treisman. 1995. The rho family GTPases RhoA, Rac1, and CDC 42Hs regulate transcriptional activation by SRF. *Cell.* 81:1159–1170.
11. Kozma, R., S. Ahmed, A. Best, and L. Lim. 1995. The ras-related protein CDC-42Hs and bradykinin promote formation of peripheral actin microspikes and filopodia in Swiss 3T3 fibroblasts. *Mol. Cell. Biol.* 15:1942–1952.
12. Minden, A., A. Lin, F.-X. Claret, A. Abo, and M. Karin. 1995. Selective activation of the JNK signaling cascade and c-jun transcriptional activity by the small GTPases Rac and CDC42Hs. *Cell.* 81:1147–1157.
13. Ridley, A.J., and A. Hall. 1994. Signal transduction pathways regulating Rho-mediated stress fibre formation: requirement for a tyrosine kinase. *EMBO (Eur. Mol. Biol. Organ.) J.* 13: 2600–2610.
14. Juliano, R.L., and S. Haskill. 1993. Signal transduction from the extracellular matrix. *J. Cell Biol.* 120:577–585.
15. Miyamoto, S., H. Teramoto, O.A. Coso, J.S. Gutkind, P.D. Burbelo, S.K. Akiyama, and K.M. Yamada. 1995. Integrin function: molecular hierarchies of cytoskeletal and signaling molecules. *J. Cell Biol.* 131:791–805.
16. Sekine, A., M. Fujiwara, and S. Narumiya. 1998. Asparagine residue in the rho gene product is the site for botulinum ADP-ribosylation. *J. Biol. Chem.* 264:8602–8605.
17. Indik, Z.K., C. Kelly, P. Chien, A.I. Levinson, and A.D. Schrieber. 1991. Human FcRII, in the absence of other Fc receptors, mediates a phagocytic signal. *J. Clin. Invest.* 88: 1766–1771.
18. Grinstein, S., and W. Furuya. 1986. Characterization of the amiloride sensitive Na^+/H^+ antiport of human neutrophils. *Am. J. Physiol.* 250:C283–C291.
19. Grynkiewicz, G., M. Poenie, and R.Y. Tsien. 1985. A new generation of $Ca2^+$ indicators with greatly improved fluorescence properties. *J. Biol. Chem.* 260:3440–3450.
20. Bouvier, G., A.M. Benoliel, C. Foa, and P. Bongrand. 1994. Relationship between phagosome acidification, phagosome-lysosome fusion, and mechanism of particle ingestion. *J. Leukocyte Biol.* 55:729–734.
21. Pitt, A., L.S. Mayorga, P.D. Stahl, and A.L. Schwartz. 1992. Alterations in the protein composition of maturing phagosomes. *J. Clin. Invest.* 90:1978–1983.
22. Nobes, C.D., and A. Hall. 1995. Rho, Rac and Cdc42 GTPases regulate the assembly of multimolecular focal complexes associated with actin stress fibers, lamellipodia, and filopodia. *Cell.* 81:53–62.
23. Swanson, J.A., and C. Watts. 1995. Macropinocytosis. *Trends. Cell Biol.* 5:424–428.
24. Rosales, C., and E. Brown. 1991. Two mechanisms for IgG Fc-receptor–mediated phagocytosis by human neutrophils. *J. Immunol.* 146:3937–3944.
25. Wilsson, A., H. Lundqvist, M. Gustafsson, and O. Stendahl. 1996. Killing of phagocytosed *Staphylococcus aureus* by human neutrophils requires intracellular free calcium. *J. Leukocyte Biol.* 59:902–907.

26. Zimmerli, S., M. Majeed, M. Gustavsson, O. Stendahl, D.A. Sanan, and J.D. Ernst. 1996. Phagosome-lysosome fusion is a calcium-independent event in macrophages. *J. Cell Biol.* 132: 49–61.
27. Di Virgilio, F., B.C. Meyer, S. Greenberg, and S.C. Silverstein. 1988. Fc receptor–mediated phagocytosis occurs in macrophages at exceedingly low cytosolic Ca^{2+} levels. *J. Cell Biol.* 106:657–666.
28. Theler, J., D.P. Lew, M.E. Jaconi, K. Krause, C.B. Wollheim, and W. Schlegel. 1995. Intracellular pattern of cytosolic $Ca2^{+}$ changes during adhesion and multiple phagocytosis in human neutrophils. Dynamics of intracellular Ca^{2+} stores. *Blood.* 85:2194–2201.
29. Greenberg, S., P. Chang, and S.C. Silverstein. 1994. Tyrosine phosphorylation of the subunit of Fc receptors, p72syk, and paxillin during Fc receptor-mediated phagocytosis in macrophages. *J. Biol. Chem.* 269:3897–3902.
30. Zalavary, S., O. Stendahl, and T. Bengtsson. 1994. The role of cyclic AMP, calcium and filamentous actin in adenosine modulation of Fc receptor-mediated phagocytosis in human neutrophils. *Biochim. Biophys. Acta.* 1222:249–256.
31. Park, J.G., R.K. Murray, P. Chien, C. Darby, and A.D. Schreiber. 1993. Conserved cytoplasmic tyrosine residues of the gamma subunit are required for a phagocytic signal mediated by Fc gamma RIIIA. *J. Clin. Invest.* 92:2073–2079.
32. Young, J.D., S.S. Ko, and Z.A. Cohn. 1984. The increase in intracellular free calcium associated with IgG gamma Zb/gamma 1 Fc receptor-ligand interactions: role in phagocytosis. *Proc. Natl. Acad. Sci. USA.* 81:5430–5434.
33. Pfefferkorn, L.C., J.G. van de Winkel, and S.L. Swink. 1995. A novel role for IgG-Fc. Transductional potentiation for human high affinity Fc gamma receptor (Fc gamma R1) signaling. *J. Biol. Chem.* 270:8164–8171.
34. Trowbridge, I.D. 1991. Endocytosis and signals for internalization. *Curr. Opin. Cell Biol.* 3:634–641.
35. Trowbridge, I.D., J.F. Collawn, and C.R. Hopkins. 1993. Signal-dependent membrane protein trafficking in the endocytic pathway. *Annu. Rev. Cell Biol.* 9:129–161.
36. Daro, E., P. Van der Sluijs, T. Galli, and I. Mellman. 1996. Rab 4 and cellubrevin define different early endosome populations on the pathway of transferrin receptor recycling. *Proc. Natl. Acad. Sci. USA.* 93:9559–9564.
37. Lamaze, C., T.H. Chuang, L.J. Terlecky, G.M. Bokoch, and S.L. Schmid. 1996. Regulation of receptor-mediated endocytosis by Rho and Rac. *Nature (Lond.).* 382:177–179.
38. Aktories, K., S. Braun, S. Rosener, I. Just, and A. Hall. 1989. The Rho gene product expressed in *E. coli* is a substrate for botulinum ADP-ribosyltransferase C3. *Biochem. Biophys. Res. Commun.* 158:209–213.
39. Aktories, K. 1997. Bacterial toxins that target Rho proteins. *J. Clin. Invest.* 99:827–829.
40. Chardin, P., P. Boquet, P. Madaule, M.R. Ropoff, E.J. Rubin, and D.M. Gill. 1989. The mammalian G protein rho C is ADP-ribosylated by *Clostridium botulinum* exoenzyme C3 and affects actin microfilaments in vero cells. *EMBO (Eur. Mol. Biol. Organ.) J.* 8:1087–1097.
41. Koch, G., J. Norgauer, and K. Aktories. 1994. ADP ribosylation of the GTP binding protein Rho by *Clostridium limosum* exoenzyme affects basal, but not *N*-formyl-peptide–stimulated, actin polymerization in human myeloid leukemic (HL60) cells. *Biochem. J.* 299:775–779.
42. Aepfelbacher, M., M. Essler, E. Huber, A. Czech, and P.C. Weber. 1996. Rho is a negative regulator of human monocyte spreading. *J. Immunol.* 157:5070–5075.
43. Jalink, K., E.J. van Croven, T. Hengeveld, N. Morii, S. Narumiya, and W.H. Moolenaar. 1994. Inhibition of lysophosphatidate and thrombin induced neurite retraction and neuronal cell rounding by ADP ribosylation of the small GTP-binding protein Rho. *J. Cell Biol.* 126:801–807.
44. Aepfelbacher, M. 1995. ADP-ribosylation of Rho enhances adhesion of U937 cells to fibronectin via the alpha 5 beta 1 integrin receptor. *FEBS (Fed. Eur. Biochem. Soc.) Lett.* 363: 78–80.
45. Hotchin, N.A., and A. Hall. 1995. The assembly of integrin adhesion complexes requires both extracellular matrix and intracellular rho/rac GTPases. *J. Cell Biol.* 131:1857–1865.
46. Sastry, S.K., and A.F. Horwitz. 1994. Integrin cytoplasmic domains: mediators of cytoskeletal linkages and extra- and intracellular initiated transmembrane signaling. *Curr. Opin. Cell Biol.* 5:819–831.
47. Gilmore, A.P., and K. Burridge. 1995. Cell adhesion-cryptic sites in vinculin. *Nature (Lond.).* 373:197–200.
48. Burbelo, P.D., S. Miyamoto, A. Utani, S. Brill, K.M. Yamada, A. Hall, and Y. Yamada. 1995. p190-B, a new member of the rho GAP family, and rho are induced to cluster after integrin cross linking. *J. Biol. Chem.* 270:30919–30926.
49. Yoshida, M., W.F. Westlin, N. Wang, D.E. Ingber, A. Rosenzweig, N. Resnick, and M.A.J. Gimbrone. 1996. Leukocyte adhesion to vascular endothelium induces E-selectin linkage to the actin cytoskeleton. *J. Cell Biol.* 13:445–455.
50. Kinch, M.S., J.L. Strominger, and C. Doyle. 1993. Cell adhesion mediated by CD4 and MHC class II proteins requires active cellular processes. *J. Immunol.* 151:4552–4561.